Available online at www.sciencedirect.com

SciVerse ScienceDirect

Ceramics International 39 (2013) 8355–8362

CERAMICS INTERNATIONAL

www.elsevier.com/locate/ceramint

Porous silicon nitride ceramics designed for bone substitute applications

Katarína Bodišová[a,*], Monika Kašiarová[b], Magdaléna Domanická[a], Miroslav Hnatko[a], Zoltán Lenčéš[a], Zuzana Varchulová Nováková[c], Ján Vojtaššák[c], Sylvia Gromošová[d], Pavol Šajgalík[a]

[a]*Institute of Inorganic Chemistry, Slovak Academy of Science, Dúbravská cesta 9, 842 36 Bratislava, Slovakia*
[b]*Institute of Materials Research, Slovak Academy of Sciences, Watsonova 47, 04353 Košice, Slovakia*
[c]*Institute of Medical Biology and Clinical Genetics, Faculty of Medecine, Comenius University, Sasinkova 4, Bratislava, Slovakia*
[d]*Associated Tissue Bank of Faculty of Medecine of P.J. Šafárik University and L. Pasteur Faculty Hospital, Triedna SNP 1, Košice, Slovakia*

Received 9 January 2013; received in revised form 19 March 2013; accepted 5 April 2013
Available online 23 April 2013

Abstract

Porous silicon nitride ceramics having properties similar to the human trabecular bone have been sintered and characterized in order to develop a material applicable as bone substitute. At first, human trabecular bone was characterized especially in terms of pore structure which is, besides the non-toxicity, the most critical for acceptation of the substitute. The pore network of highly porous trabecular bone is formed by interconnected large pores of approximately 300–1000 μm. Similar pore structure of silicon nitride-based ceramics was attained by the replica method with polyurethane sponge as pore forming agent. Porous ceramics were prepared in two ways, namely as air-sintered silicon nitride and sintered reaction-bonded silicon nitride. The materials were characterized using the same methods as for the human bone samples. Both types of ceramic materials fulfilled the microstructural requirements for bioapplications. Moreover, their non-cytotoxicity was proved by measuring the yellow tetrazolium MTT proliferation assay using human fibroblast cell line.

Keywords: B. Porosity; C. Mechanical properties; D. Si_3N_4; E. Biomedical applications

1. Introduction

The bone substitutes are commonly used for filling and reconstructing bone cavities or areas of bone loss that are caused by bone diseases or trauma [1–3]. The best results were obtained by using autologous graft, but this approach is often complicated by donor morbidity and limited amount of bone graft. On the other hand the application of more available allografts is hazardous in term of diseases transmission [4]. Nowadays, there are many synthetic bone grafts on the market, especially bioactive ceramics based on calcium phosphates characterised by profitable osteoconductivity. Nevertheless, low mechanical properties, particularly the high brittleness, make this type of substitutes unsuitable for high-load application. Aluminium and zirconium oxide ceramics or their composites which are frequently used for these applications represent particular solution of this problem, but there is still a need of even tougher and more reliable ceramic materials with subclinical ware rates [5,6].

Silicon nitride-based ceramics are well known for their superior combination of fracture toughness and hardness [7]. These are key properties for excellent wear resistance, which, combined with inertness, turns this material a suitable candidate also for high-load medical applications. Therefore most studies are focused on dense silicon nitride with the aim to replace metal alloys used in hip and knee prosthesis [5,8–10]. Besides dense silicon nitride-based ceramics also the porous form is intensively studied for bioapplications. Porous silicon nitride with a structure resembling that of cancellous bone is already commercially used as a spinal fusion implant with bone ingrowth rates similar to those reported for porous titanium. The results of studies on bone growth in porous

*Corresponding author. Tel.: +421 2 59410440; fax: +421 2 59410444.
E-mail address: uachkbod@savba.sk (K. Bodišová).

0272-8842/$ - see front matter © 2013 Elsevier Ltd and Techna Group S.r.l. All rights reserved.
http://dx.doi.org/10.1016/j.ceramint.2013.04.015

structures implanted to animals suggest that porous silicon nitride is applicable for implants requiring direct, biological skeletal fixation [5,11].

The ceramic bone substitutes should mimic the mineral part of the bone. It is known that bone is a composite of mineral phase, calcium phosphate-based hydroxyapatite, embedded in an organic matrix of collagen protein. From macroscopic point of view, the human bone has two parts—the relatively dense marginal part of the bone, called cortical bone and the internal highly porous part called trabecular or cancellous bone. For that reason the microstructure of materials designed for bio-applications, mainly for bone substitution is of great importance, besides non-toxicity and inertness or resorbability. In principle there should be a three-dimensional (3-D) interconnected porous network with interconnected large pores (more than 100 μm) enabling tissue ingrowth and nutrition delivery and also a presence of smaller pores (< 50 nm), promoting cell adhesion and adsorption of biologic metabolites [12]. Under suitable conditions the bone grows into such porous structure at a rate of ~1 μm per day [13–15].

There are many ways reported on the preparation of ceramic materials with interconnected macroporous structure, e.g. replica method using polymeric sponge or other porous materials [16], introduction of different pore-forming agents which are burnt out by calcination [17], foaming [18] or the production of gas bubbles [19]. This study deals with the preparation of ceramic structures with relatively large pores and whereas the bone structure reminds of sponge, the replica method using polyurethane sponge was chosen as appropriate [20].

The bone, despite of its relatively low density and high porosity should form tough and protective load-bearing framework of the body. Therefore, characterization of the mechanical properties of bone such as elastic modulus, strength, and fracture toughness are crucial not only in the field of medicine, but also in material research dealing with the development of bone substitutes. Elastic modulus of bone reflects its stiffness during elastic deformation and the strength presents the ability of bone to withstand the load without fracture.

The reported values of the mechanical properties of bone cover a wide range because the densities varied noticeably in relation to the type of bone and also to donor's age. Therefore the mechanical properties are frequently expressed as a function of density [21]. However, density is not the only factor influencing the properties of cancellous bone. The microstructure can also vary considerably in dependence on the part of the body from highly anisotropic to essentially isotropic [22], which significantly affects both compression strength and elastic modulus. Moreover, the applied methods of sample storage and testing conditions cause additional variation of measured data [23]. In order to minimize the influence of mentioned effects on the mechanical characteristics of bone, we have decided to measure the mechanical properties of the trabecular bone samples and the produced ceramic materials with the same testing methods and conditions. Nanoindentation was selected as a testing method, beacuse it is an effective technique to characterise biomaterials with hierarchical structure, allowing the measurement of properties at the micro or nanometer scale. It is a reliable method to assess the intrinsic mechanical properties of the single bone structural unit such as the single lamellae or trabeculae [24]. The interpretation of the results of micro-mechanical properties in connection to the macroscopic behaviour of porous materials requires a special attention and appropriate approach should be used to estimate the relation between nanoindentation measurement and macroscopic behaviour of material [25–27], including the influence of porosity [28–30].

However, the aim of this work was not to determine the properties of bone and porous ceramics on the macroscopic level from the measured nanoindentation data, but to have simple method to compare the properties of prepared porous ceramic materials by two different methods with the properties of trabecular bone.

This study is focused on the characterization of trabecular bone and subsequent preparation of porous ceramic material based on silicon nitride with microstructure and mechanical properties similar to the bone. Moreover, the biotoxicity of prepared materials will be tested.

2. Experimental

The samples of human trabecular bone (only sterilised in alcohol) and demineralised bone matrix (treated 2 h in 0.5 M HCl) were obtained from tissue bank (Associated Tissue Bank in Košice, Slovakia). The donor was approximately 40 years old without any grave disease in anamnesis.

The silicon nitride-based samples were prepared by replica method using polyurethane sponge as pore-forming agent by two different methods. In the first one, suspension with 35 vol % of Si_3N_4 powder (Yantai, Tomley Hi-Tech Ind. & Tra. Co., Ltd., d_{90}=10.0 μm, O < 1.5%) was prepared. Deionised water was used as a liquid medium and for optimum dispersion 0.022 g of dispersant was added per gram of powder. The suspension was homogenized for 24 h by ball milling with Si_3N_4 milling balls. The polyurethane sponges were dipped into slurry and compressed while submerged, to fill all the cells in the sponge and achieve good wetting between sponge and slurry. The impregnated sponge was then passed through rollers to remove the excess suspension. After drying the sponge was burnt out at 600 °C for 1 h in air (heating rate: 1 °C min^{-1}). The subsequent sintering was also performed in air at 1250 °C; the heating rate was 10 °C min^{-1} and the cooling rate 20 °C min^{-1}. These samples are depicted as air-sintered silicon nitride (ASSN).

In the second method sintered reaction bonded silicon nitride (SRBSN) samples were prepared. Suspension with 48 wt% of powder mixture consisting of silicon (grade 4D, d_{50}=7 μm, Sicomill, Vesta Ceramics AB, Ljungaverk, Sweden) and α-Si_3N_4 (SN-E10, Ube Ind., Japan) in a weight ratio of 3:1 was prepared in deionised water. For optimum dispersion 0.07 g of dispersant was added per gram of powder. The suspension was homogenized for 24 h by ball milling with Si_3N_4 milling balls. The polyurethane sponges were impregnated and burnt out similarly as in the previous case. The nitridation of Si-based porous structure was carried out at 1400 °C for 3 h followed by sintering at 1750 °C for 2 h in nitrogen atmosphere.

The densities of samples were measured by mercury immersion. X-ray microtomography (GE Phoenix/X-Ray nanotom 180) was used to characterize the structure of large pores. The average width of large pores was determined from the width of pores or pore channels measured on the slices from XRD microtomography using Atlas software. For each sample at least 100 pores or pore channels were evaluated on 15–20 slices. The pore size distribution of smaller pores was determined by mercury intrusion porosimetry (Pore Master 60). The phase composition of sintered Si_3N_4-based samples was investigated by powder X-ray diffraction (Bruker AXS D8 Discover X-ray diffractometer). The amount of oxygen in samples was measured using ONH analyzer (EMGA 830, Horiba Jobin Ivon). EDS analysis (JEOL JSM-7600F/EDS/WDS/EBSD) was used to determine the differences in chemical composition of trabecular bone and demineralised bone.

Samples of porous Si_3N_4 were prepared in the form of discs with the diameter 25 mm and thickness 5 mm. The sample surfaces were polished with diamond suspension to the final polishing of 1 μm. Trabecular bones were received in the form of rectangular specimens with dimensions of $10 \times 10 \times 10$ mm^3. Samples were polished using SiC papers (800, 1200, 2400 grit) with final polishing by 4000 grit SiC paper corresponding to the grain size of 5 μm. Instead of water, ethylene glycol was used for polishing in order to eliminate the demineralization of bone [31].

Table 1
Apparent densities of natural bone and demineralised bone samples.

	Natural bone (g cm^{-3})	Demineralised bone (g cm^{-3})
Sample 1	0.29	0.16
Sample 2	0.89	0.65
Sample 3	1.14	0.97

Measurements of the hardness and elastic modulus were carried out by the micro/nanohardness tester (CSM TTX NHT2) with the Berkovich indentor. Standard loading-unloading cycle with the maximum load of 100 mN and loading rate 200 mN/min was used. The holding time was 10 s at the maximum load. Indentation hardness and elastic modulus were calculated according to Oliver and Pharr method [32]. Fifty indentation measurements were performed at different location of the samples.

Compressive strength was measured using Lloyds Instruments apparatus with the cross-head speed of 1 mm/min. The average value was calculated from the data obtained from ten samples.

Cytotoxicity of prepared materials was estimated according to proliferation tested by applying the MTT-test (methyl thiazolyl tetrazolium). The MTT test is a colorimetric test that measures cell survival as a percentage of survival of untreated controls. MTT (3-(4,5-dimethylthiazol-2-yl)-2,5-diphenyltetrazolium bromide, called also yellow tetrazole) is a soluble tetrazolium salt that is cleaved in viable cells by active mitochondrial

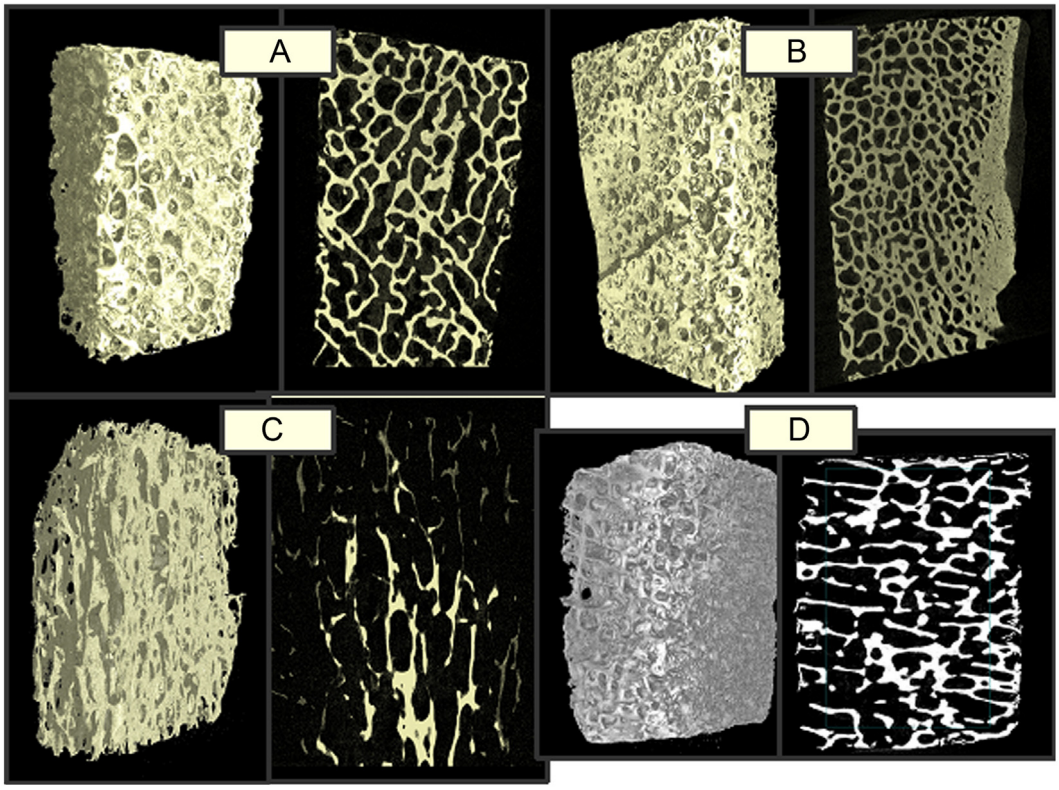

Fig. 1. XRD microtomography of demineralised bone matrix with porosity of 70 vol% (A), 58 vol% (B), 91 vol% (C) and natural bone with 64 vol% of porosity (D).

dehydrogenases forming blue or purple insoluble formazan crystals. Human fibroblast cells were pipetted into a well of the 96-well microplate in amount of 10^4 cells. Then, various concentrations of powdered Si_3N_4-based samples (0.1, 1, 5, 10, 25, 50, and 100%) were added. After 72 h MTT salt (Promega) was added followed by 3 h incubation. Wells were then aspirated, and acid isopropanol (4% 1 mol/L HCl in 2-isopropanol) was added to each. The cell proliferation was evaluated on microreader ELISA by measuring the absorbance at 490 nm wavelength.

Table 2
Average pore size (APS) of natural bone and demineralised bone matrix with different porosities (NM=not measured).

	Natural trabecular bone		Demineralised trabecular bone	
	Porosity (vol%)	APS (μm)	Porosity (vol%)	APS (μm)
Sample 1	64	750 ± 250	69.5	820 ± 220
Sample 2	NM	NM	57.9	420 ± 150
Sample 3	NM	NM	90.8	850 ± 230

3. Results and discussion

3.1. Bone characterization

The bone tissue differs strongly in dependence on the type of bone, donor age, etc. For density measurement three bone samples and three demineralised bone samples with evidently different densities were chosen, to have an overview on the cross section of bone from the lowest to the highest density (Table 1). It is important to mention that the marginal part of samples with the highest densities was already a part of cortical

Table 3
Mechanical properties of natural trabecular bone and demineralised trabecular bone.

	Trabecular bone	Demineralised trabecular bone
Hardness (GPa)	0.51 ± 0.03	0.54 ± 0.03
Young's modulus (GPa)	11.2 ± 0.9	11.7 ± 0.5
Compressive strength (MPa)	4.1 ± 1.9	2.7 ± 1.3

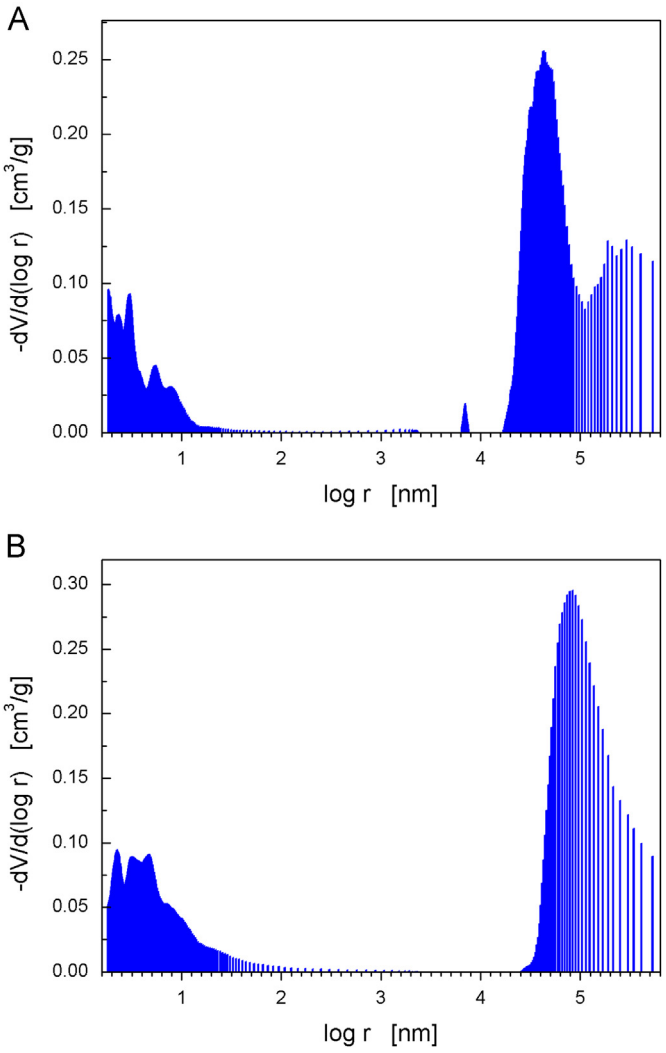

Fig. 2. Pore size distribution of bone (A) and demineralised bone matrix (B) measured by mercury intrusion porosimetry.

bone. Samples with the lowest densities were from the very porous area of trabecular bone.

Despite the wide range of values it can be concluded that the densities of demineralised bone samples are slightly lower than those of the natural bone. EDS analysis proved certain decrease of calcium and phosphorus content in the bone treated in HCl acid compared to natural bone. The decrease can be explained by the reaction of HCl acid with the main inorganic compound of bone—hydroxyapatite, thereby forming calcium chloride and phosphoric acid. The decomposition of hydroxyapatite is inevitably accompanied by slight density decrease and also certain mechanical weakening could be expected. Despite these negative influences the acid treatment was necessary to get the demineralized bone matrix by the acid extraction of allografts. The remaining biological material generally contains collagen type I, non-collagenous proteins and osteoinductive growth factors, the latter having very significant role for the acceptation of natural allograft after transplantation [4]. For that reason it was necessary to characterise also the demineralised bone samples.

X-ray microtomography was used to visualize and characterize the porosity of bone and demineralised bone matrix (DBM). The obtained structures are shown in Fig. 1. The structure of bone is very porous and consists of interconnected porous network. The average width of pores was evaluated and the results for three samples of DBM and one for natural bone are summarized in Table 2. The width of interconnected pore channels is generally in the range from 300 μm to 1000 μm depending on the overall porosity, with lower values for denser bone samples.

More precise results were provided by mercury immersion porosimetry. Pore-size distributions of natural bone with density of 1.1 g cm^{-3} and DBM with density of 0.65 g cm^{-3} are depicted in Fig. 2. The majority of pore volume consists of large pores in the range of 40−1000 μm for natural bone and from 80 μm to 1000 μm for DBM. However, significant part of pores falls into meso and microporous region (< 50 nm). There are only few pores in the range of 200 nm–30 μm.

The measured data of hardness and Young's modulus of natural bone and DMB are summarized in Table 3, and are in accordance with the data reported in literature [33,34]. Regarding the result of the compressive strength, the strength of trabecular bone is 4.1 MPa with relatively high scatter. It is caused by the variation of the porosity of tested trabecular bone (see Table 2). The values of strength are consistent with the values of compressive strength of trabecular bone which is typically around 2–12 MPa [21]. The compressive strength of the demineralized bone is slightly lower 2.7 MPa again with high value of standard deviation. Whereas the measured mechanical properties for both types of samples do not differ markedly, it could be concluded that the demineralization process was provided at relatively mild conditions which are sufficient for protein uncovering, but did not noticeably affect the mechanical properties of the bone.

3.2. Characterization of porous ceramics

Preliminary experiments showed that the both types of ceramics—air sintered silicon nitride (ASSN) and sintered reaction bonded silicon nitride (SRBSN) can be prepared by replica method with densities in the range of 0.5 to 1.5 g cm^{-3} in dependence on the amount of infiltrated suspension. For further characterization only the samples of approximate density 0.8–1.1 g cm^{-3} (corresponding to 65–75% of total porosity) were selected with the aim to imitate the structural properties of bone.

The phase composition of prepared samples was evaluated from the X-ray diffraction patterns. The main phase was α-Si_3N_4, independently on the preparation and sintering technique and both types of samples also contained a certain amount of β-Si_3N_4. The sintering in air resulted in partial oxidation of silicon nitride. Silicon oxide, formed on the surface of silicon nitride grains, acts as a sintering aid and provides some densification at relatively low temperatures. Based on the results of XRD and oxygen elemental analysis (~5 wt% O), silicon oxide was mostly present in amorphous form, because only very weak cristobalite peaks were observed on the XRD pattern (1–2% determined by TOPAS profile and structure analysis software). The presence of cristobalite is rather undesirable because of relatively large thermal expansion coefficient (11.4×10^{-6} °C^{-1} [35]) which can induce crack formation on the sample surface during cooling.

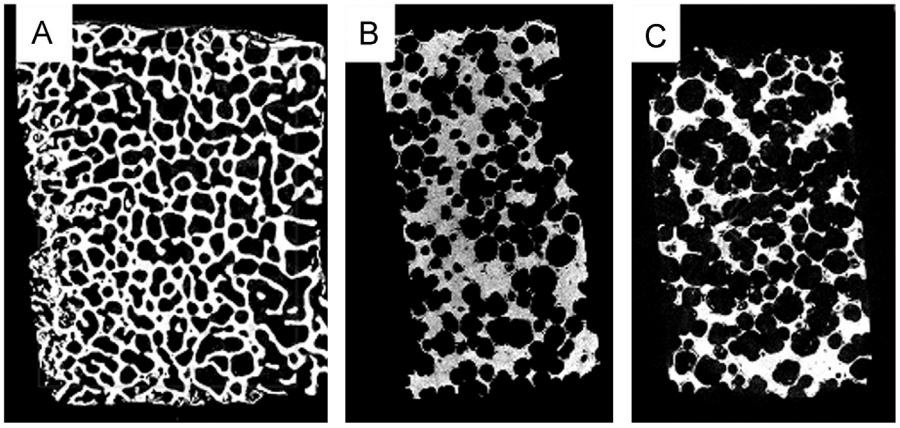

Fig. 3. Sections from XRD microtomography of bone (64 vol% pores)—(A), air-sintered Si_3N_4 (65 vol% pores)—(B), SRBSN (73 vol% pores)—(C).

In the case of SRBSN samples β-SiC is the only phase besides Si_3N_4. Silicon carbide is formed during the sintering process due to the high carbon activity in the used graphite resistance furnace. However, no negative influence of SiC is expected. Nanoparticles of SiC might have even mild positive effect on the mechanical properties of porous ceramics and also cytocompatibility of SiC was already successfully tested [36].

The microstructure of the ceramic materials was visualized similarly to the bones by X-ray microtomography (Fig. 3). After sponge burn out an interconnected porous network was formed in the ceramic materials. The character of pores is rather different from those in bones; namely the pores possess regular circular section instead of irregularly shaped pores in bones. However, the width of the pore channels in ceramics is in good agreement with the width of pores in bones (Table 4). Consequently, two microstructural requirements, i.e. interconnected macroporous network with sufficiently large pores are fulfilled for both types of prepared silicon nitride-based ceramics.

Table 4
Average pore size (APS) of silicon nitride-based ceramics.

	Porosity (vol%)	APS (μm)
ASSN	65	720 ± 190
SRBSN	73	750 ± 200

Similar conclusion could be drawn from the porosimetry results (Fig. 4). Both Si_3N_4-based samples contain significant fraction of large pores above the diameter of 100 μm. However, the fraction of mesopores is markedly lower than in human bone (Fig. 2), especially in the case of SRBSN samples.

The mechanical properties of trabecular bone and prepared ceramics are presented in Table 5. Because the properties were measured using nano-indentation technique, the values reflect only the properties of ceramic or bone matrix without the contribution of large pores, i.e. the skeletal structure. The results show that the hardness and Young's modulus of air-sintered silicon nitride is very close to the values measured for bone with the same technique. On the contrary, SRBSN samples exhibit values higher by one order of magnitude. It could be attributed to the relatively high densification of the Si_3N_4 matrix and to a certain extent also to the presence of SiC particles (E=440 GPa). Although the measured properties are

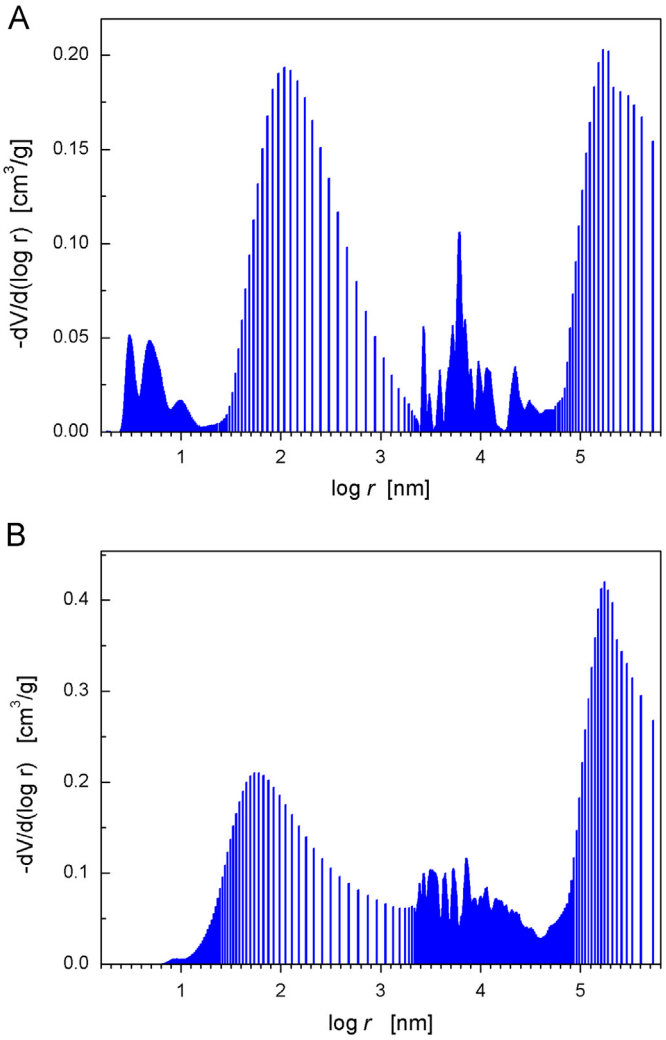

Fig. 4. Pore size distribution of air-sintered Si3N4 (A) and SRBSN (B) measured by mercury intrusion porosimetry.

Table 5
Mechanical properties of bone and ceramic samples.

	Bone	ASSN	SRBSN
Hardness (GPa)	0.51 ± 0.03	0.46 ± 0.07	6.3 ± 2.3
Young's modulus (GPa)	11.2 ± 0.9	11.4 ± 0.9	92.1 ± 21.3
Compressive strength (MPa)	4.1 ± 1.9	2.9 ± 0.4	7.5 ± 1.5

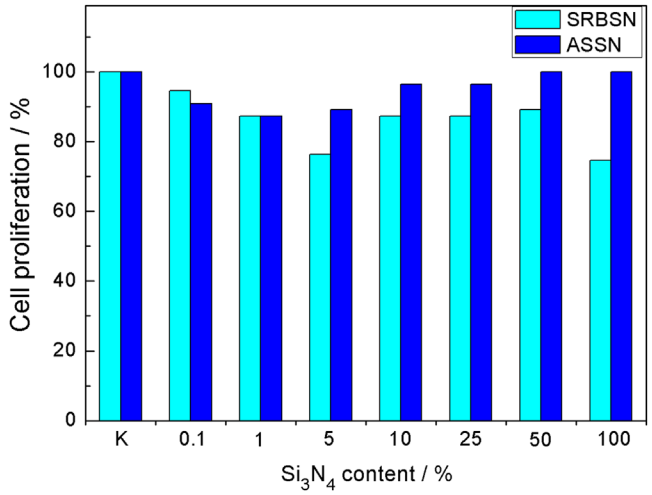

Fig. 5. MTT test of sintered reaction bonded silicon nitride and air-sintered silicon nitride tested at various concentrations of the samples. The cell survival results are expressed as percentage of cells in control medium (K), without the addition of Si_3N_4.

higher compared to bone, it does not definitely mean that this preparation method (SRBSN) is inappropriate for bone substitutes. Hardness and Young's modulus could be modified to values closer to the bone, especially by lowering the sintering temperature or shortening the sintering time.

The compressive strength of prepared silicon nitride based materials does not significantly deviate from the values of the trabecular bones. The compressive strength of the air sintered silicon nitride was 2.9 ± 0.4 MPa, it means slightly lower than that of the bone. The mean value of compressive strength of SRBSN was 7.5 ± 1.5 MPa. The measured values of the strength of porous silicon nitride materials are comparable with the values of other already well-established ceramic biomaterials based on Al_2O_3 and ZrO_2 [37–41] and confirms that the prepared silicon nitride materials have high potential to be used for the bio-application as bone substitute. It is necessary to point out that big difference in the elastic modulus or strength between bone and ceramic substitute leads to the greater stress concentration and fracture at the bone–ceramic interface. This is the reason why it is so important to prepare the materials with the mechanical properties similar to trabecular bone.

The effects of porous silicon nitride based ceramics materials on human fibroblast viability were measured by MTT test. As it was mentioned, MTT is a yellow water-soluble tetrazolium dye which is reduced by living cells to an insoluble purple formazan product in aqueous solutions. The amount of formazan generated is directly proportional to the number of viable cells. The non-cytotoxicity of porous silicon nitride-based ceramic materials was confirmed by this MTT proliferation test, because the percentage of proliferation was above 70% in all cases (Fig. 5). Based on these results we can conclude that porous silicon nitride-based ceramic materials show no significant antiproliferative effect after 24 h and 72 h incubation.

4. Conclusion

The pore structure of human trabecular bone and demineralised bone was examined by X-ray tomography and mercury immersion method. Subsequently, porous silicon nitride-based ceramics with structure similar to the trabecular bone structure consisting of interconnected macroporous network was prepared using replica method. The pore size distribution in the most important dimensional regions, i.e. under 50 nm and over 100 μm was similar to that of the bone, especially in the air-sintered silicon nitride ceramics. Likewise, the mechanical properties of air-sintered silicon nitride were very close to the bone properties. In the case of sintered reaction-bonded silicon nitride the preparation method requires further optimization in terms of enhancing the meso- and nano-pores content and decrease the hardness and Young's modulus values. The non-cytotoxicity of porous silicon nitride-based ceramic materials was confirmed by MTT proliferation test.

Acknowledgment

This study was supported by the Technology Assistance Agency under the Contract no. APVV-0500-10 and partly by Grant of the Ministry of Health of the Slovak Republic No. 2007/36-UK-07.

References

[1] M.D. Brown, T.I. Malinin, P.B. Davis, A roentgenographic evaluation of frozen allografts versus autografts in anterior cervical spine fusions, Clinical Orthopaedics 119 (1976) 231–236.
[2] G.E. Friedlaender, Current concepts review: bone-banking, Journal of Bone and Joint Surgery American 64 (1982) 307–311.
[3] V.M. Steelman, Creutzfeld–Jakob disease recommendations for infection control, American Journal of Infection Control 22 (1994) 312–318.
[4] G. Zimmermann, A. Moghaddam A, Allograft bone matrix versus synthetic bone graft substitutes, Injury: International Journal of the Care of the Injured 42 (2011) S16–S21.
[5] B.S. Bal, M.N. Rahaman, Orthopedic applications of silicon nitride ceramics, Acta Biomaterialia 8 (2012) 2889–2898.
[6] A. Neumann, M. Kramps, Ch. Ragoß, H.R. Maier, K. Jahnke, Histological and microradiographic appearances of silicon nitride and aluminum oxide in a rabbit femur implantation model, Materialwissenschaft und Werkstofftechnik 35 (2004) 569–573.
[7] J. Dusza, P. Šajgalík, Fracture toughness and strength testing of ceramic composites, in: N.P. Cheremisinoff, P.N Cheremisinoff (Eds.), Handbook of Advanced Materials Testing, Marcel Dekker Inc., New York, 1995, pp. 399–436.
[8] B.S. Bal, A. Khandkar, R. Lakshminarayanan, I. Clarke, A.A. Hoffman, M.N. Rahaman, Testing of silicon nitride ceramic bearings for total hip arthroplasty, Journal of Biomedical Materials Research Part B 87 (2008) 447–454.
[9] C.C. Guedes e Silva, B. König, M.J. Carbonari, M. Yoshimoto, S. Allegrini, J.C. Bressiani, Tissue response around silicon nitride implants in rabbits, Journal of Biomedical Materials Research 84A (2008) 337–343.

[10] M. Mazzocchi, A. Bellosi, On the possibility of silicon nitride as a ceramic for structural orthopaedic implantans. Part I: processing, microstructure, mechanical properties, cytotoxicity, Journal of Materials Science: Materials in Medicine 19 (2008) 2881–2887.
[11] M.C. Anderson, R. Olsen, Bone ingrowth into porous silicon nitride, Journal of Biomedical Materials Research 92 (2010) 1598–1605.
[12] P. Sepulveda, J.R. Jones, L.L. Hench, Bioactive sol–gel foams for tissue repair, Journal of Biomedical Materials Research 59 (2002) 340–348.
[13] A.A. Hofmann, R.D. Bloebaum, K.N. Bachus, Progression of human bone ingrowth into porous-coated implants, Acta Orthopaedica Scandinavica 68 (1997) 161–166.
[14] R.D. Bloebaum, K.N. Bachus, N.G. Momberger, A.A. Hofmann, Mineral apposition rates of human cancellous bone at the interface of porous coated implants, Journal of Biomedical Materials Research 28 (1994) 537–544.
[15] A.A. Hofmann, R.D. Bloebaum, K.E. Koller, A. Lahav, Does celecoxib have an adverse effect on bone remodeling and ingrowth in humans?, Clinical Orthopaedics and Related Research 452 (2006) 200–204
[16] J. Saggio-Woyansky, C.E. Scott, Processing of porous ceramic, Journal of American Ceramic Society Bulletin 71 (1983) 1674–1682.
[17] D-M. Liu, Fabrication of hydroxyapatite ceramic with controlled porosity, Journal of Materials Science: Materials in Medicine 8 (1997) 227–232.
[18] M.D.M. Innocentini, P. Sepulveda, V.R. Salvini, V.C. Pandolfelli, J. R. Coury, Permeability and structure of cellular ceramics: A comparison between two preparation techniques, Journal of the American Ceramic Society 81 (1998) 3349–3352.
[19] E. Ryshkewitch, Compressive strength of porous sintered alumina and zirconia, Journal of the American Ceramic Society 36 (1953) 65–68.
[20] R.A. Studart, J.L. Gauckler, E. Tervoort, Processing route to macroporous ceramics: a review, Journal of the American Ceramic Society 89 (2006) 1771–1789.
[21] D.R. Carter, W.C. Hayes, Bone compressive strength: the influence of density and strain rate, Science 194 (1976) 1174–1176.
[22] E.D. Dyson, C.K. Jackson, W.J. Whitehouse, Scanning electron microscope studies of human trabecular bone, Nature 225 (1970) 957–959.
[23] S.A. Goldstein, The mechanical properties of trabecular bone: dependence on anatomic location and function, Journal of Biomechanics 20 (1987) 1055–1061.
[24] S. Hengsberger, P. Ammann, B. Legros, R. Rizzoli, P. Zysset, Intrinsic bone tissue properties in adult rat vertebrae: modulation by dietary protein, Bone 36 (2005) 134–141.
[25] T.N. Shepherd, J. Zhang, T.C. Ovaert, R.K. Roeder, G.L. Niebur, Direct comparison of nanoindentation and macroscopic measurements of bone viscoelasticity, Journal of the Mechanical Behavior of Biomedical 4 (2011) 2055–2062.
[26] S. Hengsberger, J. Enstroem, F. Peyrin, P. Zysset, How is the indentation modulus of bone tissue related to its macroscopic elastic response? A validation study, Journal of Biomechanics 36 (2003) 1503–1509.
[27] D.R. Carter, W.C. Hayes, The compressive behavior of bone as a two-phase porous material, Journal of Bone & Joint Surgery 59A (1977) 954–962.
[28] I. Sevostianov, M. Kachanov, Impact of the porous microstructure on the overall elastic properties of the osteonal cortical bone, Journal of Biomechanics 33 (2000) 881–888.
[29] Z. Fan, J.G. Swadener, J.Y Rho, M. Roy, G.M. Pharr, Anisotropic properties of human tibial cortical bone as measured by nanoindentation, Journal of Orthopaedic Research 20 (2000) 806–810.
[30] J.G. Swadener, G.M. Pharr, Indentation of elastically anisotropic half-spaces by cones and parabolae of revolution, Philosophical Magazine A 81 (2001) 447–466.
[31] E. Donnelly, S.P. Baker, A.L. Boskey, M.C.H. van der Meulen, Effects of surface roughness and maximum load on the mechanical properties of cancellous bone measured by nanoindentation, Journal of Biomedical Materials Research Part A 77 (2006) 426–435.
[32] W.C. Oliver, G.M Pharr, An improved technique for determining hardness and elastic modulus using load and displacement sensing indentation experiments, Journal of Materials Research 7 (1992) 1564–1583.
[33] L.J. Gibson, M.F. Ashby, B.A. Harley, Cellular Materials in Nature and Medicine, Cambridge University Press, Cambridge, ISBN 978-0-521-19544-7, 2010.
[34] P.K. Zysset, X.E. Guo, C.E. Hoffler, K. Moore, S.A. Goldstein, Elastic modulus and hardness of cortical and trabecular bone lamellae measured by nanoindentation in the human femur, Journal of Biomechanics 32 (1999) 1005–1012.
[35] O. San, C. Özgür, Preparation of stabilized β-cristobalite ceramic foam from diatomite, Journal of Alloys and Compounds 484 (2009) 920–923.
[36] B. Cappi, S. Neuss, J. Salber, R. Telle, R. Knüchel, H. Fisher, Cytocompatibility of high strength non-oxide ceramics, Journal of Biomedical Materials Research Part A 93 (2010) 67–76.
[37] B.-H. Yoon, W.-Y. Choi, H.-E. Kim, J.-H. Kim, Y.-H. Koh, Aligned porous alumina ceramics with high compressive strengths for bone tissue engineering, Scripta Materialia 58 (2008) 537–540.
[38] D. Shi, G. Jiang, Synthesis of hydroxyapatite films on porous Al_2O_3 substrate for hard tissue prosthetics, Materials Science and Engineering C 6 (1998) 175–182.
[39] S.-H. An, T. Matsumoto, H. Miyajima, A. Nakahira, K.-H. Kim, S. Imazato, Porous zirconia/hydroxyapatite scaffolds for bone reconstruction, Dental Materials 28 (2012) 1221–1231.
[40] H.-W. Kim, S.-Y. Lee, C.-J. Bae, Y.-J. Noh, H.-E. Kim, H.-M. Kim, J. S. Ko, Porous ZrO_2 bone scaffold coated with hydroxyapatite with fluorapatite intermediate layer, Biomaterials 24 (2003) 3277–3284.
[41] X. He, Y.Z. Zhang, J.P Mansell, B. Su, Zirconia toughened alumina ceramic foams for potential bone graft applications: fabrication, bioactivation, and cellular responses, Journal of Materials Science: Materials in Medicine 19 (2008) 2743–2749.